

Supporting Information

Ionic gel paper with long-term bendable electrical robustness for use in flexible electroluminescent devices

Minghui He,[†] Kaili Zhang,[†] Guangxue Chen,[†] Junfei Tian,^{†} Bin Su,^{*‡}*

[†] State Key Laboratory of Pulp & Paper Engineering, South China University of Technology, Guangzhou 510640, Guangdong, P. R. China

[‡] Department of Chemical Engineering, Monash University, Clayton, Victoria 3800, Australia

* Corresponding author:

Email: jftian_scut@163.com

Email: subin0000@iccas.ac.cn

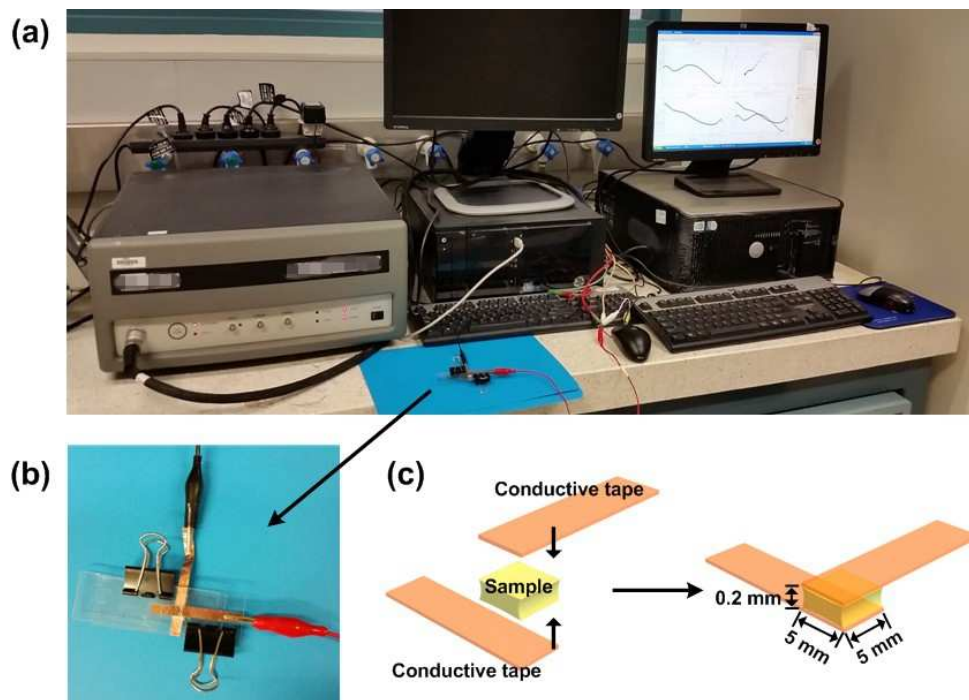


Figure S1. Electrical study of ionic gel paper (IGP). (a) Representative photograph of a sample being measured by the alternating current (AC) impedance method through an electrochemical system. (b) Photograph and (c) Schematic illustration of the details for measuring the sample. The testing condition was at room temperature, ~ 25 °C and the humidity was $\sim 35\%$.

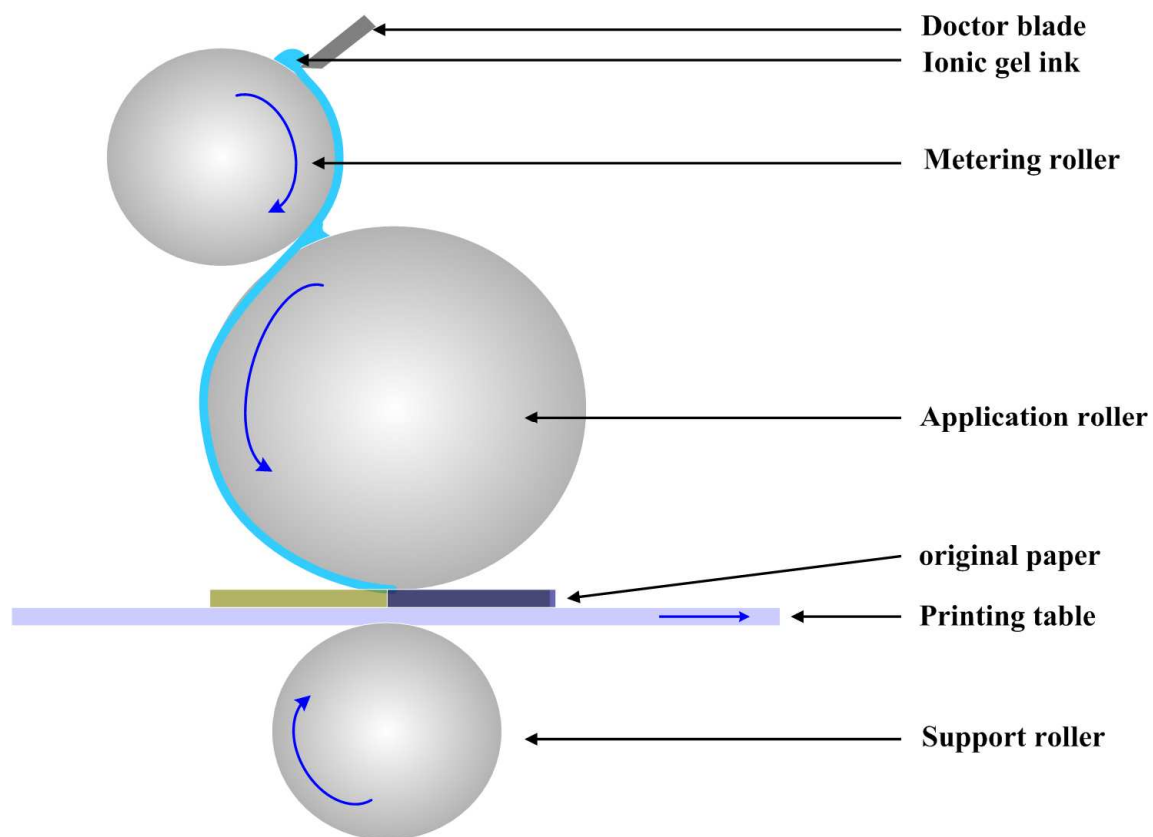


Figure S2. Schematic illustration of cross-sectional structure of the roller-to-plate (R2P) process to prepare stable and uniform IGP.

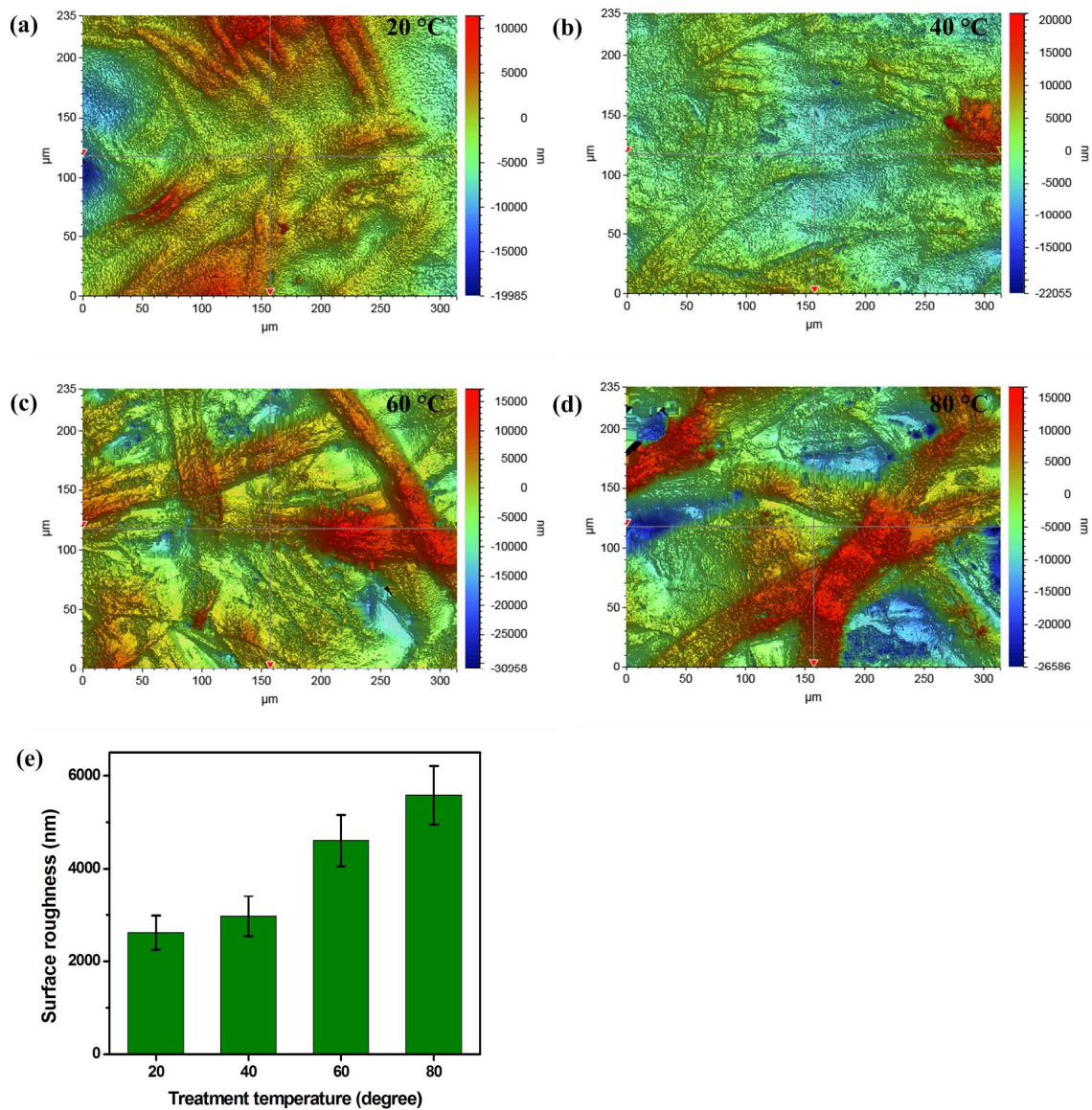


Figure S3. Heating-temperature-dependent surface roughness of IGP. 2D surface topography images from the optical profilometer of IGP treated at (a) 20 °C, (b) 40 °C, (c) 60 °C and (d) 80 °C, respectively. (e) The dependence of surface roughness of IGP on the heating temperature.

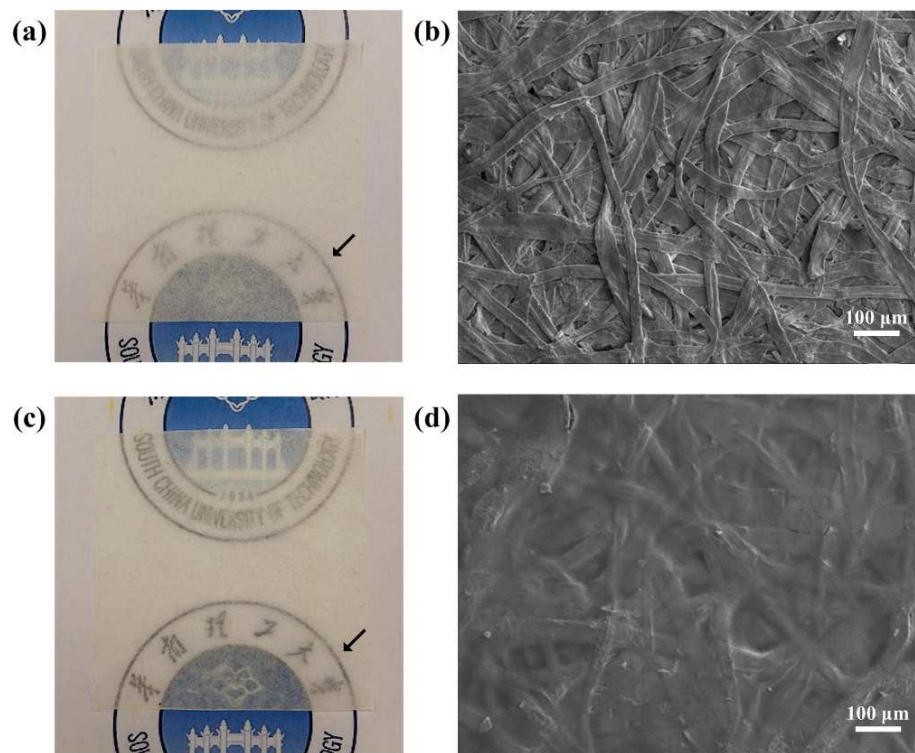


Figure S4. Physical morphologies of original paper and IGP. Digital photographs of one piece of (a) original paper and (c) IGP placed horizontally. Compared with the original paper, the IGP shows more transparent. Top view SEM images of (b) an original paper and (d) an IGP. A continuous layer of ionic gel was covered upon the cellulose fiber network of the IGP.

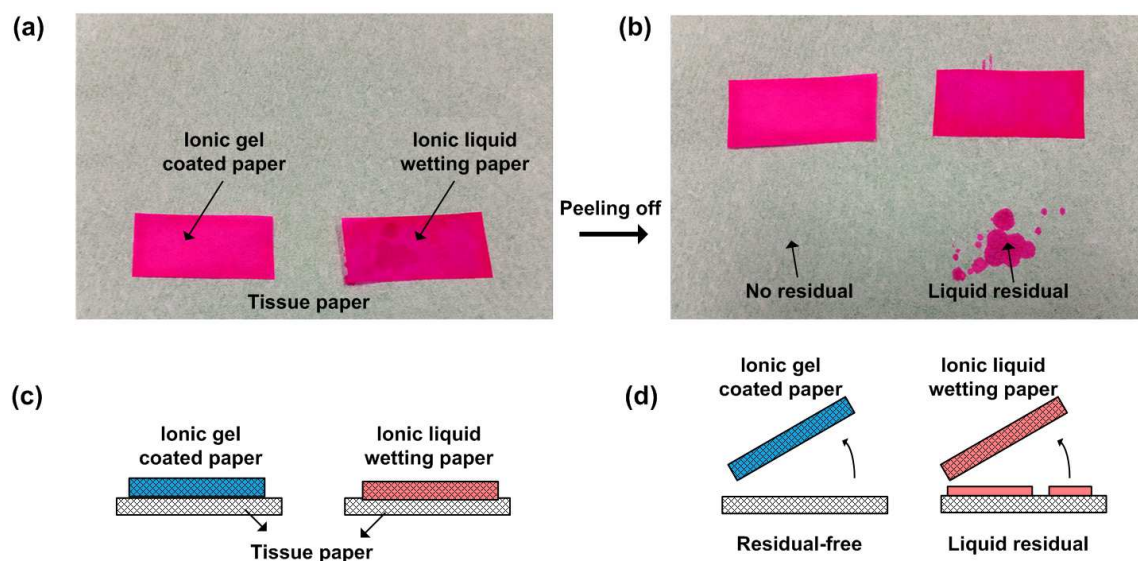


Figure S5. Residual-free advantage of IGP. (a) Representative digital image of paper filled with ionic gel (left) and ionic liquid (right) placed upon a tissue paper. Rhodamine B was used to stain ionic gel and ionic liquid to facilitate observation. (b) Representative digital image of peeling off these two paper. None of dyed spots could reside upon the tissue paper when using the IGP, indicating its residual-free advantage. On the other hand, ionic liquid was easy to flow, yielding several contamination spots when contacted with the tissue paper. (c,d) are the schematic illustrations of (a,b).

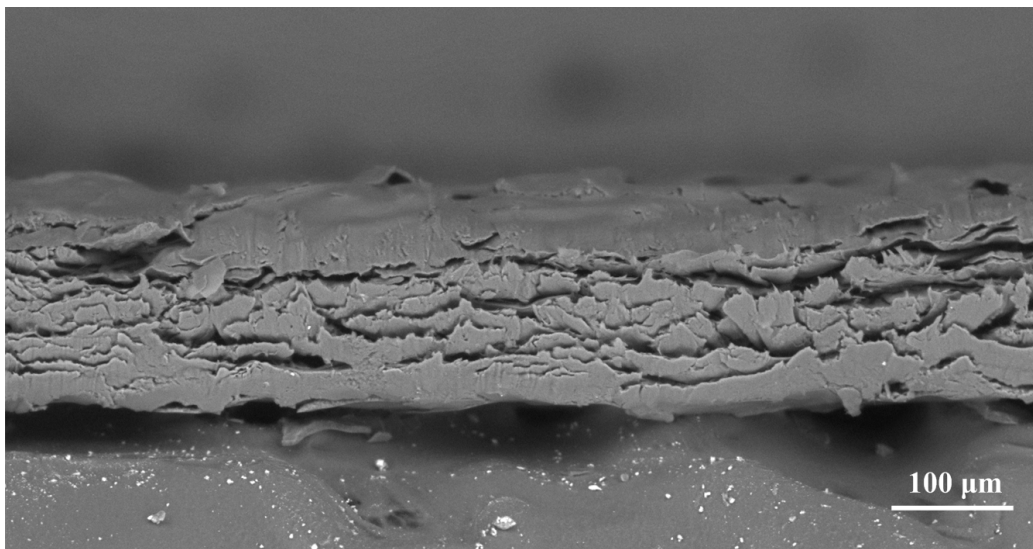


Figure S6. Cross-sectional morphology of IGP. Cross-sectional SEM image of the IGP. The ionic gels not only covered the top but also permeated inside the $\sim 200\ \mu\text{m}$ thick paper.

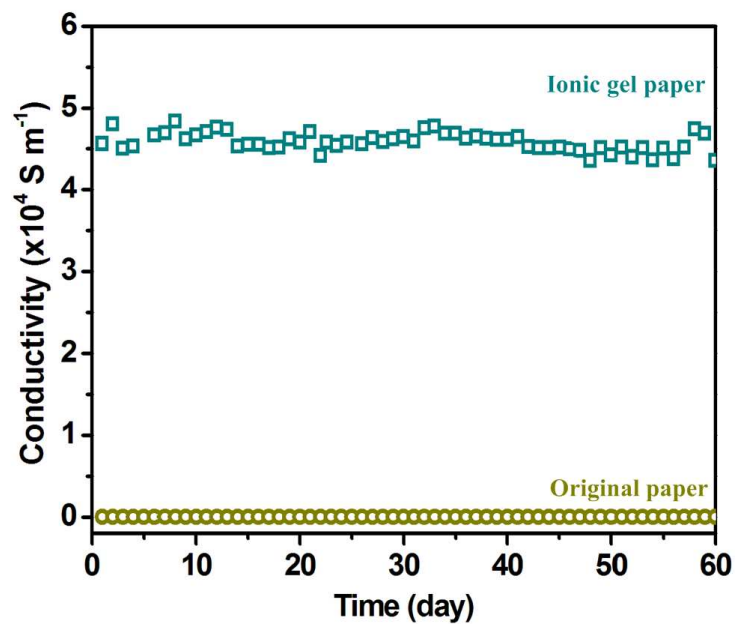


Figure S7. Long-term electrical robustness of IGP. The dependence of the conductivity of IGP (blue dots) and original paper (yellow dots) on the storage time. The testing condition was at room temperature, ~ 25 °C and the humidity was ~ 35%.

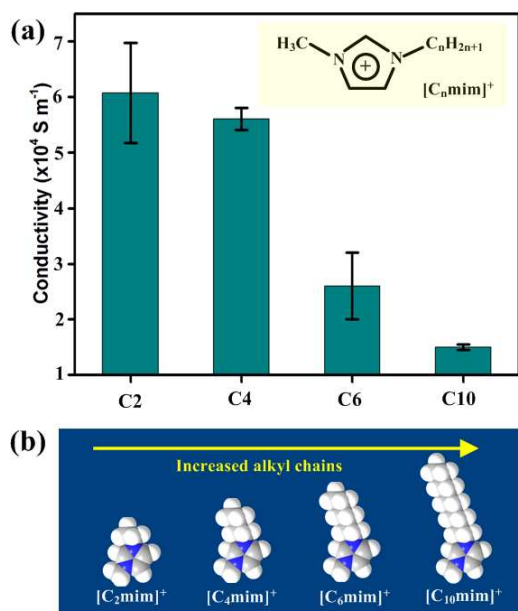


Figure S8. The increase of carbochains in the cation segment of ionic liquids led to the decrease of conductivity of IGP. a) The dependence of the conductivity of IGP on the ionic liquid species. Following the increase of the alkyl chains from C₂ to C₁₀, the conductivity of IGP was reduced accordingly. b) Chemical structures of diverse ionic liquids with increasing alkyl chains from C₂ to C₁₀.

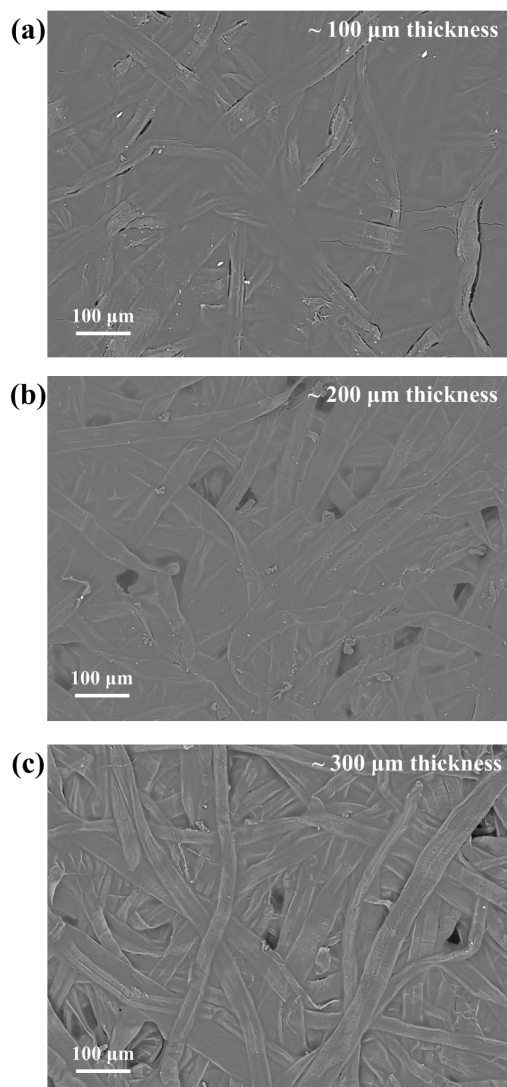


Figure S9. The morphologies of IGP prepared by original paper with diverse thicknesses. Top view SEM images of IGP by coating a similar layer of ionic gel inks onto the original paper with a) $\sim 100\ \mu\text{m}$, b) $\sim 200\ \mu\text{m}$ and c) $\sim 300\ \mu\text{m}$ thickness. Following the increase of the paper thickness, the fiber networks were more obvious. However, the change of paper thickness showed a negligible effect on the conductivity.

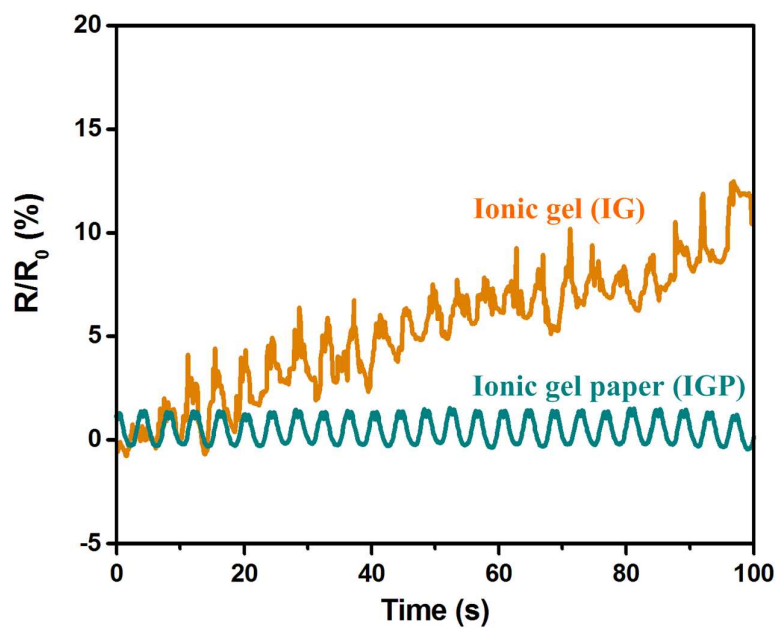


Figure S10. Comparison of electrical robustness between IG and IGP. The dependence of resistance change of the ionic gel (IG, orange line) and IGP (Green line) on the time (input frequency: 0.25 Hz) for the folding angle of 120° . The applied voltage in the electrical tests was 1 V, the relative humidity was 35 % and the temperature was 25°C .

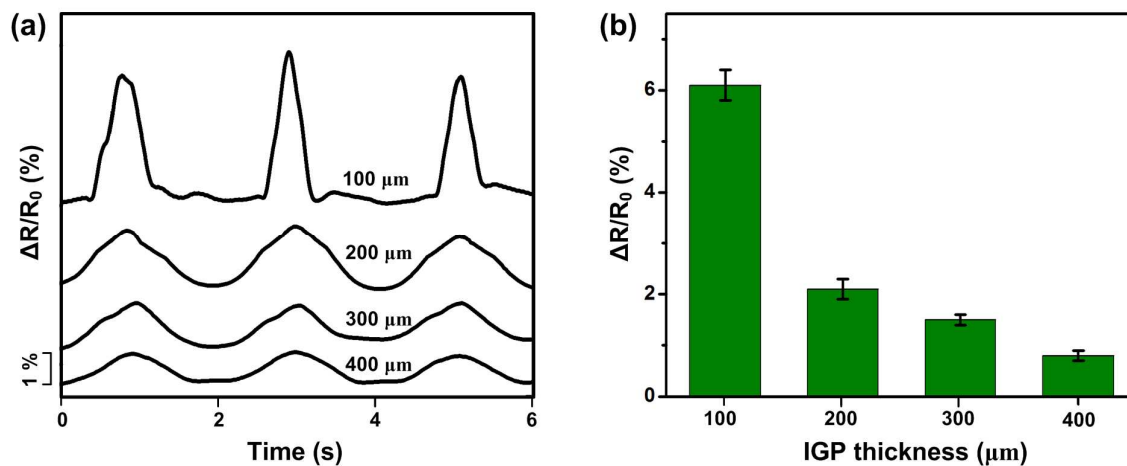


Figure S11. Electrical response of IGP with diverse paper thicknesses. (a) Plots of resistance change of IGP with diverse paper thicknesses as a function of time (folding angle: 120°). (b) The dependence of resistance change on the IGP thickness. The applied voltage in the electrical tests was 1 V, the frequency was 0.5 Hz, the relative humidity was 35 % and the temperature was 25 °C.

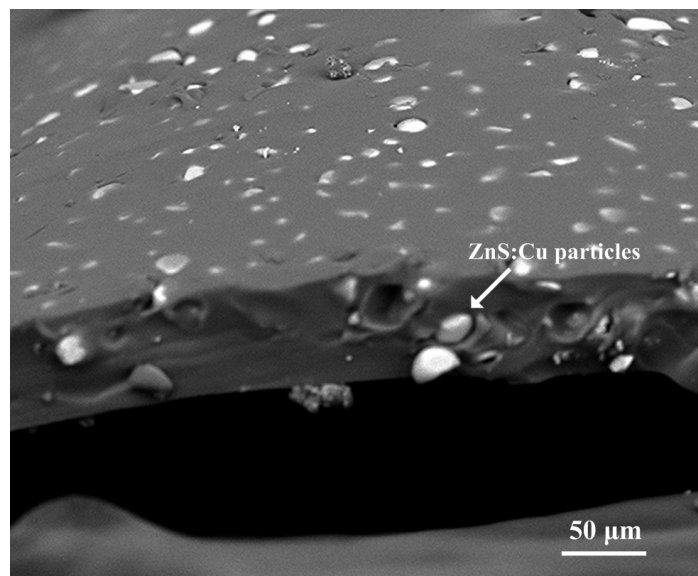


Figure S12. Cross-sectional SEM image of the ZnS:Cu emissive layer. The ZnS:Cu microparticles were homogenously dispersed in the PDMS layer and the thickness of this layer was $\sim 56 \mu\text{m}$.